Author/s:
Rybtsov, S;Sobiesiak, M;Taoudi, S;Souilhol, C;Senserrich, J;Liakhovitskaia, A;Ivanovs, A;Frampton, J;Zhao, S;Medvinsky, A

Title:
Hierarchical organization and early hematopoietic specification of the developing HSC lineage in the AGM region

Date:
2011-06-01

Citation:
Rybtsov, S., Sobiesiak, M., Taoudi, S., Souilhol, C., Senserrich, J., Liakhovitskaia, A., Ivanovs, A., Frampton, J., Zhao, S. & Medvinsky, A. (2011). Hierarchical organization and early hematopoietic specification of the developing HSC lineage in the AGM region. Journal of Experimental Medicine, 208 (6), pp.1305-1315. https://doi.org/10.1084/jem.20102419.

Persistent Link:
https://hdl.handle.net/11343/261885

Hierarchical organization and early hematopoietic specification of the developing HSC lineage in the AGM region

Stanislav Rybtsov,[1] Malgorzata Sobiesiak,[2] Samir Taoudi,[3] Céline Souilhol,[1] Jordi Senserrich,[1] Anna Liakhovitskaia,[1] Andrejs Ivanovs,[1] Jon Frampton,[4] Suling Zhao,[1] and Alexander Medvinsky[1]

[1]Institute for Stem Cell Research, Medical Research Council Centre for Regenerative Medicine, University of Edinburgh, Edinburgh EH9 3JQ, Scotland, UK
[2]Department of Internal Medicine II, Division of Hematology, Immunology, Oncology, and Rheumatology, University Clinic of Tübingen, Tübingen 72076, Germany
[3]Molecular Medicine Division, Walter and Eliza Institute of Medical Research, Melbourne, Parkville, Victoria 3052, Australia
[4]Institute for Biomedical Research, College of Medical and Dental Sciences, University of Birmingham, Birmingham B15 2TT, England, UK

The aorta-gonad-mesonephros region plays an important role in hematopoietic stem cell (HSC) development during mouse embryogenesis. The vascular endothelial cadherin$^+$ CD45$^+$ (VE-cad$^+$CD45$^+$) population contains the major type of immature pre-HSCs capable of developing into long-term repopulating definitive HSCs. In this study, we developed a new coaggregation culture system, which supports maturation of a novel population of CD45-negative (VE-cad$^+$CD45$^-$CD41$^+$) pre-HSCs into definitive HSCs. The appearance of these pre-HSCs precedes development of the VE-cad$^+$CD45$^+$ pre-HSCs (termed here type I and type II pre-HSCs, respectively), thus establishing a hierarchical directionality in the developing HSC lineage. By labeling the luminal surface of the dorsal aorta, we show that both type I and type II pre-HSCs are distributed broadly within the endothelial and subendothelial aortic layers, in contrast to mature definitive HSCs which localize to the aortic endothelial layer. In agreement with expression of CD41 in pre-HSCs, in vivo CD41-Cre–mediated genetic tagging occurs in embryonic pre-HSCs and persists in all lymphomyeloid lineages of the adult animal.

CORRESPONDENCE
Alexander Medvinsky:
A.Medvinsky@ed.ac.uk

Abbreviations used: AGM, aorta-gonad-mesonephros; HSC, hematopoietic stem cell; OG, Oregon green; sGFP, silent GFP; VE-cad, vascular endothelial cadherin; YS, yolk sac.

The aorta-gonad-mesonephros (AGM) region is an organ with complex cellular architecture in which hematopoietic stem cells (HSCs) mature during a narrow time window before liver colonization, initially within the ventral domain of the dorsal aorta (Godin and Cumano, 2002; Dzierzak and Speck, 2008; Medvinsky et al., 2011). During the functional embryonic day (E) 11.5–12.5 period when the AGM region acts as an HSC organ, the number of definitive HSCs does not exceed one to three. However, the strong autonomous HSC generation potential of the AGM region can be unveiled in explant culture (Medvinsky and Dzierzak, 1996; Kumaravelu et al., 2002). Although the embryonic endothelium is considered to be a source of definitive HSCs in the developing embryo (Zovein et al., 2008; Chen et al., 2009; Bertrand et al., 2010; Kissa and Herbomel, 2010), the exact details of this process remain unclear.

AGM explant cultures can be used to replicate the formation of definitive HSCs in the embryo and have been useful in the understanding of some mechanisms of HSC development (Medvinsky and Dzierzak, 1996; Cai et al., 2000; Robin et al., 2006); however, their usefulness for such analysis is limited. Development of an AGM reaggregation culture system allowed some essential hurdles to be overcome (Taoudi et al., 2008). Introduction of a dissociation/reaggregation step before culture enabled manipulation of cells to be performed. During 4 d of culture, definitive HSCs undergo a 150-fold expansion in a stroma-dependent manner within three-dimensional AGM reaggregates. Using the

The Rockefeller University Press $30.00
J. Exp. Med. Vol. 208 No. 6 1305-1315
www.jem.org/cgi/doi/10.1084/jem.20102419

The Journal of Experimental Medicine

reaggregation system, the population of vascular endothelial cadherin$^+$ CD45$^+$ (VE-cad$^+$CD45$^+$) pre-HSCs capable of maturing into definitive HSCs has been identified (Taoudi et al., 2008). On rare occasions, we observed the formation of HSCs from CD45$^-$ cells, which included VE-cad$^+$CD45$^-$ endothelial cells. However, because of a possibility of contamination during sorting with the major VE-cad$^+$CD45$^+$ pre-HSC population, the existence of CD45$^-$ pre-HSCs in the AGM region remained unclear. Given current views that HSCs derive from the embryonic endothelium (Zovein et al., 2008; Chen et al., 2009; Eilken et al., 2009; Lancrin et al., 2009; Bertrand et al., 2010; Boisset et al., 2010; Kissa and Herbomel, 2010), we have been looking for culture conditions that might favor the generation of definitive HSCs from the VE-cad$^+$CD45$^-$ population.

In this study, we demonstrate that replacement of the complete AGM microenvironment with a stromal OP9 line favors the development of definitive HSCs from the VE-cad$^+$CD45$^-$ cells, thus clearly identifying this population as pre-HSCs. However, the VE-cad$^+$CD45$^-$ pre-HSCs are not true endothelial cells as they are primed with a hematopoietic CD41 marker. We also show that in contrast to definitive HSCs, which are localized to the endothelial lining, pre-HSCs are broadly distributed throughout the wall of the dorsal aorta. Thus, specification of the HSC lineage in the mouse embryo involves at least two preliminary hematopoietically primed maturation steps. In accord with expression of CD41 on pre-HSCs, CD41-Cre genetically labels in vivo pre-HSCs and proportionally the adult hematopoietic system. Based on phenotypic and spatial characterization of two classes of pre-HSCs and definitive HSCs, we propose a simple model for HSC development in the AGM region.

RESULTS

Identification of the VE-cad$^+$CD45$^-$ pre-HSC population in the AGM region

For this analysis, we purified three cell populations by FACS from the E10.5 (36–39 somite pairs) and E11.5 AGM region, (a) VE-cad$^+$CD45$^+$, (b) VE-cad$^+$CD45$^-$, and (c) VE-cad$^-$CD45$^+$, and coaggregated them with OP9 cells (Fig. 1 A and Fig. S1). Coaggregates were produced by combining 1 ee (embryo equivalent) of each of these populations with 10^5 OP9 cells using centrifugation in the pipette tip, and these were then cultured as described previously (Taoudi et al., 2008; Sheridan et al., 2009). Although definitive HSCs can be detected by direct transplantation of freshly isolated cells, pre-HSCs must first mature into definitive HSCs in culture. Direct transplantation of the E10.5 AGM region does not normally give hematopoietic repopulation (Müller et al., 1994); however, the VE-cad$^+$CD45$^-$ fraction (only) gave rise to definitive HSCs in the coaggregate culture (Fig. 1, B and C). In line with previous results (North et al., 2002; Taoudi et al., 2005), the first definitive HSCs detectable by direct transplantation in the E11.5 AGM resided within the VE-cad$^+$CD45$^+$ population (Fig. 1 D). Using the complete E11.5 AGM reaggregation system, we previously identified the major VE-cad$^+$CD45$^+$ pre-HSCs as a population capable of maturation into definitive HSCs (Taoudi et al., 2005). In this study, coaggregation culture of the VE-cad$^+$CD45$^-$ population with OP9 cells resulted in the appearance of ~11 definitive HSCs with long-term multilineage engraftment potential per embryo equivalent (Fig. 1 E; Fig. 2, A, B, and E; and Fig. S2). Direct comparison confirmed the superior support of definitive HSC production by OP9 cells than by complete AGM stroma (Fig. S1 E). Coaggregation of the VE-cad$^+$CD45$^+$ population with OP9 cells gave only 4.8 HSCs per embryo equivalent (Fig. 2, C–E). Successful long-term multilineage engraftment was also observed in secondary recipients (Fig. S2). Thus, these culture conditions facilitate the formation of definitive HSCs from a VE-cad$^+$CD45$^-$ population that is distinct from previously identified VE-cad$^+$CD45$^+$ pre-HSCs. Real-time PCR analysis confirmed the lack of CD45 messenger RNA in the VE-cad$^+$CD45$^-$ population (Fig. S1 D). These experiments identify the VE-cad$^+$CD45$^-$ cells in the E11.5 AGM region as embryonic ancestors of definitive HSCs that are capable of maturing into definitive HSCs during development.

In parallel experiments, we tested whether VE-cad$^+$CD45$^-$ pre-HSCs can be identified in the E11.5 yolk sac (YS) and the fetal liver (Fig. S2 C). None of the VE-cad$^+$CD45$^-$

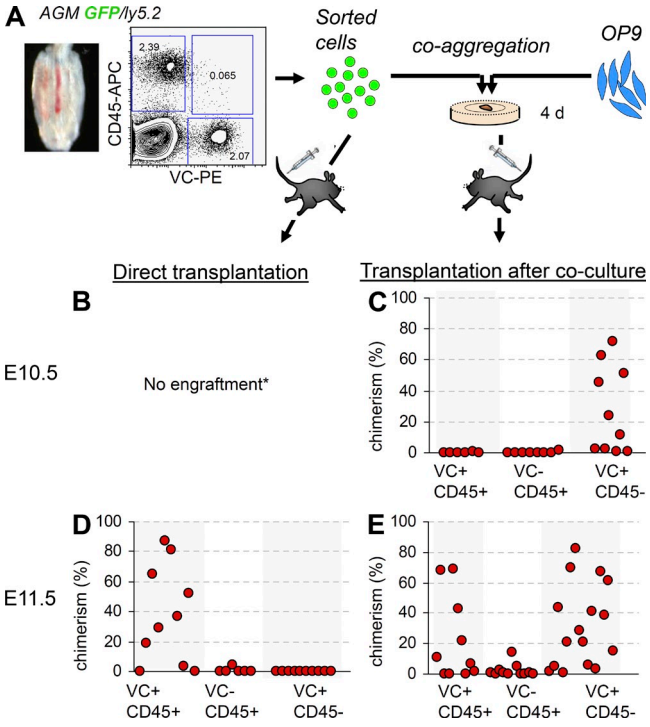

Figure 1. Identification of VE-cad$^+$CD45$^-$ pre-HSCs in the AGM region. (A) Experimental design. (B–E) E10.5 (B and C) or E11.5 (D and E) AGM regions were dissociated and sorted on the basis of CD45 and VE-cad expression. Sorted cells were either directly transplanted (B and D) or allowed to mature in coaggregate cultures with OP9 cells for 4 d and then transplanted (C and E). Transplanted doses are 2 (C), 4 (D), and 0.2 ee (E) per recipient. Chimerism (percentage) indicates the proportion of donor-derived cells in the blood of recipient animals. Data are derived from three independent experiments for each type of experiment in C–E. (B) *, see Muller et al. (1994). VC, VE-cad.

populations purified from these sources gave rise to definitive HSCs after co-culture with OP9 stromal cells (Fig. 2 F). 1 out of 11 recipients transplanted with YS-derived VE-cad$^+$CD45$^-$ cells showed short-term repopulation at high level (19%), which disappeared by 3.5 mo after transplantation (not depicted).

VE-cad$^+$CD45$^-$ pre-HSCs mature into definitive HSCs via the intermediate VE-cad$^+$CD45$^+$ pre-HSC phenotype

Subsequently, we studied the dynamics of the pre-HSC to definitive HSC transition by transplanting coaggregates after 24, 48, 72, and 96 h of culture into irradiated recipients (Fig. 3 A). We observed that VE-cad$^+$CD45$^-$ cells matured into definitive HSCs slightly slower than VE-cad$^+$CD45$^+$ pre-HSCs.

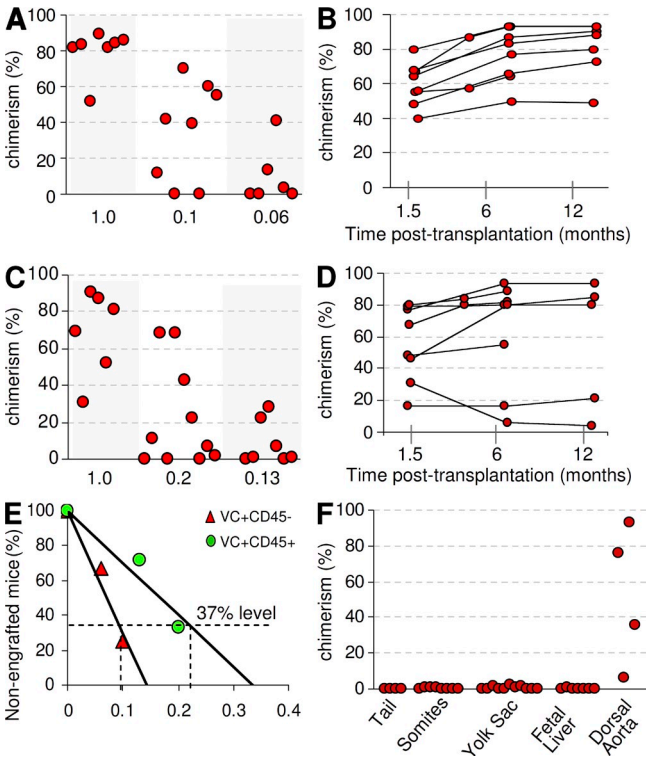

Figure 2. Quantification of definitive HSCs in coaggregate cultures of the E11.5 AGM region. (A, C, and E) Quantification of definitive HSCs from coaggregate cultures using limiting dilution analysis. (A–D) HSC generation by the VE-cad$^+$CD45$^-$ population (A and B) and the VE-cad$^+$CD45$^+$ population (C and D) is shown. 1 ee of the population of interest was aggregated with OP9 cells, and the resulting population was transplanted into each recipient (A, C, and E) at the indicated dose expressed in embryo equivalents (x axis). Each red dot represents one recipient mouse. (B and D) Kinetics of donor-derived blood chimerism upon transplantation of coaggregate cultures of VE-cad$^+$CD45$^-$ (B) or VE-cad$^+$CD45$^+$ (D) populations. Each recipient mouse received 1 ee of donor-derived cells. Time after transplantation (months) is indicated. (F) Coaggregates were made with VE-cad$^+$CD45$^-$ cells from E11.5 YS, fetal liver, and nonhematopoietic tissues (tail and somites) and transplanted (2 ee/recipient). Control coaggregates of the dorsal aorta were transplanted at 0.2 ee/recipient. Data are derived from three independent experiments for each type of experiments in A–E and two independent experiments for F. VC, VE-cad.

One possible explanation for this is that VE-cad$^+$CD45$^-$ pre-HSCs are more immature and pass via an extra step to become HSCs. To test this directly, VE-cad$^+$CD45$^-$ cells sorted to a high level of purity that excludes any significant presence of VE-cad$^+$CD45$^+$ cells (Fig. S3, A and B) were co-cultured with OP9 cells for 24 h. Cells derived from the VE-cad$^+$CD45$^-$ population were then repurified to obtain VE-cad$^+$CD45$^+$ and VE-cad$^+$CD45$^-$ cell populations (Fig. 3 B, sorting II; and Fig. S3 C). These populations were again coaggregated with fresh OP9 cells and cultured for 4 d to allow them to complete maturation into definitive HSCs and then transplanted into irradiated recipients (Fig. S3, D and E). Importantly, the VE-cad$^+$CD45$^-$ population (a) does not contain definitive HSCs (Figs. 1 B and 3 A; Taoudi et al., 2005) and (b) does not mature into definitive HSCs during the first 48 h of co-culture (Fig. 3 A). Only the resorted VE-cad$^+$CD45$^+$ fraction but not the VE-cad$^+$CD45$^-$ fraction matured into definitive HSCs by the end of the co-culture period (Fig. 3 B). Thus, within the first 24 h of co-culture with OP9 stroma, the initial VE-cad$^+$CD45$^-$ pre-HSCs acquired the VE-cad$^+$CD45$^+$ (pre-HSC) phenotype. These experiments establish a hierarchy for the developing definitive HSC lineage within the AGM region, indicating that VE-cad$^+$CD45$^-$ pre-HSCs mature into definitive HSCs via the intermediate VE-cad$^+$CD45$^+$ pre-HSC phenotype. Based on these observations, we define VE-cad$^+$CD45$^-$ and VE-cad$^+$CD45$^+$ cells as type I and type II pre-HSCs, respectively.

Type I pre-HSCs are CD41$^{+/low}$Lin$^-$

To characterize type I pre-HSCs further, we included additional surface markers in our experiments. The VE-cad$^+$CD45$^-$ population contains endothelial cells and is highly enriched for vascular tubule–forming cells (Taoudi et al., 2005). Surprisingly, however, we found that the VE-cad$^+$CD45$^-$ population also contains a proportion of cells that express B220, CD3e, and Ter119 (and less convincingly Mac1, CD4, and GR1), cumulatively called here Lin$^+$ (Fig. S4). We tested whether the type I pre-HSCs reside within the VE-cad$^+$CD45$^-$Lin$^+$ or VE-cad$^+$CD45$^-$Lin$^-$ fraction (Fig. S4 A). After coaggregation and culture with OP9 cells, the cultures were assayed in the long-term repopulation assay, revealing that only the VE-cad$^+$CD45$^-$Lin$^-$ cells were capable of developing into definitive HSCs (Fig. S4, B and C).

We then investigated whether the type I pre-HSCs express CD41, a marker expressed in all hematopoietic progenitors in early embryos (Corbel and Salaün, 2002; Emambokus and Frampton, 2003; Mikkola et al., 2003), and a fraction of cells in E9.5–10.5 embryos that are capable of developing into adult HSCs upon injection into newborn recipients (Ferkowicz et al., 2003). Approximately 10% of cells within the VE-cad$^+$CD45$^-$ population express CD41 at various levels (Fig. 4 A). The VE-cad$^+$CD45$^-$ population was purified into (a) CD41^{high}, (b) CD41^{low}, and (c) CD41$^-$ fractions and cultured in coaggregates with OP9 cells. We found that only the VE-cad$^+$CD45$^-$CD41^{low} population is capable of maturing into definitive HSCs. Truly endothelial VE-cad$^+$CD45$^-$CD41$^-$

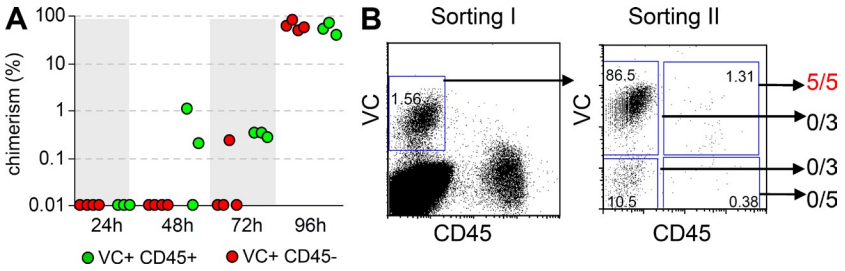

Figure 3. In the E11.5 AGM region, VE-cad$^+$CD45$^-$ (type I) pre-HSCs mature into definitive HSCs via intermediate VE-cad$^+$CD45$^+$ (type II) pre-HSCs. (A) Time course of appearance of definitive HSCs during 4 d of culture. In each experiment, 1 ee of AGM cells was aggregated with OP9 cells and transplanted into each recipient at each time point. (B) Sorted VE-cad$^+$CD45$^-$ cells co-cultured with OP9 cells for 24 h were resorted on the basis of VE-cad (VC) and CD45 expression. All four resorted populations were coaggregated with fresh OP9 cells and cultured for a further 96 h and transplanted separately into irradiated recipients (2 ee/recipient). Numbers of mice repopulated/transplanted are indicated. Data are derived from two independent experiments.

cells did not generate definitive HSCs (Fig. 4 B). An in vitro assay confirmed that, in contrast to the VE-cad$^+$CD45$^-$CD41$^-$ cells, the VE-cad$^+$CD45$^-$CD41^{low} fraction was devoid of the endothelial potential (Fig. 5), which is in agreement with previous observations that CD41 expression marks commitment to hematopoietic cells during development (Li et al., 2005; Hashimoto et al., 2007).

We then tested by direct transplantation whether CD41 also marks definitive HSCs from freshly isolated AGM regions. In line with a previous study (McKinney-Freeman et al., 2009), we found that, with one exception, only recipients of CD41^{low} cells were repopulated (Fig. 4, D and E), demonstrating that CD41 is indeed expressed on AGM definitive HSCs.

Type I and type II pre-HSCs are localized to both luminal and subluminal layers of the dorsal aorta

To determine the localization of the definitive HSCs and pre-definitive HSCs, the fluorescent dye Oregon green (OG) was microinjected into the lumen of dorsal aorta using a micropipette for 30 s (Fig. 6, A and B; and Fig. S5). This allowed us to label aortic luminal endothelial and hematopoietic cells and, to a lesser extent, the immediate subluminal cell layer but not the deeper underlying mesenchyme (Fig. 6, C–F). All cells in intra-aortic clusters were labeled, indicating that intercellular contacts are loose enough in intra-aortic clusters to allow OG penetration. The basal lamina underlying the endothelial lining is possibly a stronger barrier for OG penetration. After 30 s of labeling, a cell suspension was prepared, and OG-labeled and unlabeled cells were purified by FACS and directly transplanted into irradiated recipients (Fig. 6, G, H, J, and K). Donor repopulation was only observed in mice that received

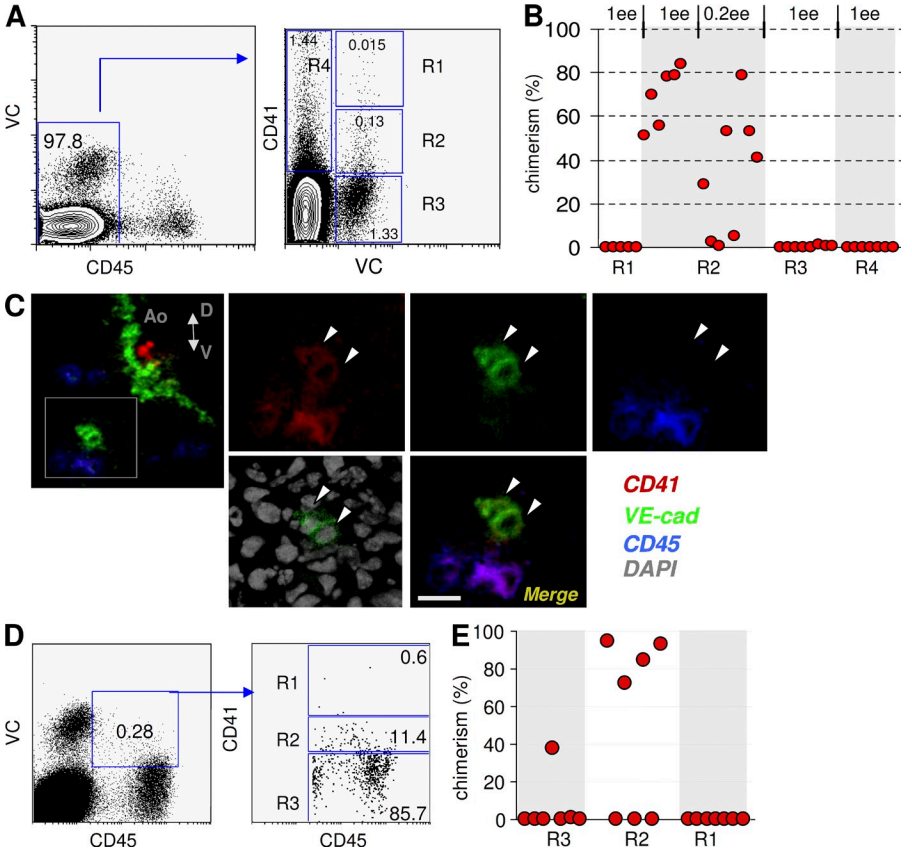

Figure 4. In the E11.5 AGM region, CD41 marks type I pre-HSCs and definitive HSCs. (A) Gating strategy for fractionating the VE-cad$^+$CD45$^-$ population into CD41^{high} (R1, 46 ± 4/ee), CD41^{low} (R2, 260 ± 18/ee), and CD41$^-$ (R3, 2300 ± 110/ee) subsets. R4 includes the VE-cad$^-$CD45$^-$CD41$^+$ cell population. (B) Recipients were transplanted with sorted populations R1, R2, R3, and R4 after 4-d co-culture with OP9 cells (doses per recipient indicated). (C) AGM region immunostaining for type I pre-HSCs (VE-cad$^+$CD45$^-$CD41$^+$). The boxed area within the top left image is shown at high magnification with individual stainings for VE-cad, CD41, or CD45 (top right). Merged images are shown for DAPI and VE-cad (bottom left) and VE-cad, CD41, and CD45 (bottom right). Arrowheads show subluminal localization of these cells. D↔V, dorsoventral orientation. Bar, 10 µm. (D) Gating strategy for subfractionating definitive HSCs on the basis of CD41 expression. (E) VE-cad$^+$CD45$^+$ cells sorted on the basis of CD41 expression (high, R1; low, R2; and negative, R3) from the uncultured AGM region were directly transplanted into irradiated recipients (4 ee/recipient). The CD41^{low} fraction contained HSCs. Data are derived from three independent experiments for all experiments. VC, VE-cad.

transplants of VE-cad$^+$CD45$^+$OG^{high} cells but not those transplanted with VE-cad$^+$CD45$^+$OG$^{-/low}$ cells, indicating that definitive HSCs in the AGM region are localized to the endothelial lining of the dorsal aorta (Fig. 6 K). This result is in agreement with previous data using Sca1-GFP reporter mice (de Bruijn et al., 2002).

We then determined whether type I pre-HSCs localized to the luminal endothelium of the dorsal aorta. To this end, purified VE-cad$^+$CD45$^-$OG^{high}, VE-cad$^+$CD45$^-$OG^{low}, and VE-cad$^+$CD45$^-$OG$^-$ populations were coaggregated with OP9 cells to test their capacity to develop into definitive HSCs. Long-term repopulation assays showed that all three VE-cad$^+$CD45$^-$ populations developed into definitive HSCs (Fig. 6 I). The intensity of OG staining determined by flow cytometry was correlated with staining on confocal images, thereby defining the localization of type I pre-HSCs within luminal, immediate subluminal, and deeper subluminal areas of the dorsal aorta (Fig. 6, E and F). However, the assessment of exact position of OG low cells below the luminal aortic layer may not be considered very accurate, except that they are located under the first luminal layer and that OG-negative cells must be localized comparatively deeper. Further confocal analysis revealed rare VE-cad$^+$CD45$^-$CD41$^+$ cells integrated both in the luminal endothelial lining and intra-aortic clusters (unpublished data), which is in agreement with a recent study (Yokomizo and Dzierzak, 2010), and in the subluminal compartment of the dorsal aorta (Fig. 4 C and Fig. S6).

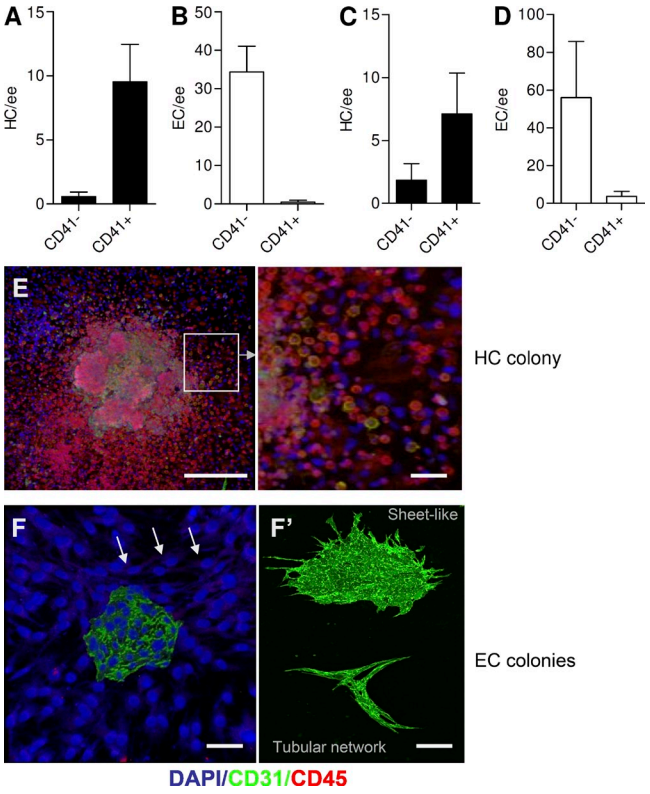

Figure 5. Lack of endothelial activity in the VE-cad$^+$CD41$^+$ population. (A–D) E10.5 (A and B) and E11.5 (C and D) AGM VE-cad$^+$CD45$^-$ populations were purified based on CD41 expression. Error bars show standard deviation of three independent sorting experiments. (A–F) Hematopoietic (A, C, and E) and endothelial (B, D, and F) in vitro assays were set up in 96-well plates using single-cell deposition. (E and F) Hematopoietic (E) and endothelial (F) colonies were stained for CD31 and CD45. DAPI was used to visualize nuclei. Arrows show OP9 cells used as feeders. Bars: (E, left) 200 µm; (E, right) 30 µm; (F and F′) 25 µm. Bar graphs show absolute number of hematopoietic colonies per embryo equivalent (HC/ee; A and C) or endothelial colonies per embryo equivalent (EC/ee; B and D). All data are derived from three independent experiments.

Previous analysis led us to a supposition that type II (VE-cad$^+$CD45$^+$) pre-HSCs are organized predominantly in large intra-aortic clusters (Taoudi et al., 2008). Here, we found that both luminal (OG positive) and subluminal (OG negative) VE-cad$^+$CD45$^+$ cells were capable of developing into definitive HSCs in coaggregate cultures (Fig. 6 L). Accordingly, confocal analysis demonstrated the presence of rare VE-cad$^+$CD45$^+$ cells, usually organized in small clusters, under the luminal surface of the dorsal aorta (Fig. S7). Thus, both type I and type II pre-HSCs are integrated not only in the luminal endothelial lining of the dorsal aorta, as was proposed previously for type II pre-HSCs (Taoudi et al., 2008), but also within its deeper layers.

Expression of Cre from a CD41-driven transgene labels the adult hematopoietic system

CD41-Cre mice (Emambokus and Frampton, 2003) were crossed with silent GFP (sGFP) mice (Gilchrist et al., 2003), and recombination resulting in GFP expression was assessed in the adult hematopoietic system. Labeling of hematopoietic cells in these embryos was observed before onset of circulation, beginning from E8 concurrently in preliver sites of hematopoiesis: the YS, allantois, and dorsal aorta (Figs. 7 and 8 A), which later harbor HSCs (Medvinsky et al., 2011). Interestingly, labeling of cells in the allantois continued to its base and extends to the proximal part of the bifurcated dorsal aorta (Fig. 7 B). By E8.5, labeling of cells in the paired dorsal aorta spread further rostrally (Fig. 7 C). At E9.5–10.5, GFP$^+$ cells actively circulated in the vascular system (Fig. 7, D and E; and not depicted). By E11.5, GFP$^+$ cells colonized the liver (Fig. 7 F). In contrast to previous observations (Emambokus and Frampton, 2003), we found efficient (between 35 and 60%) labeling of adult blood and hematopoietic tissues (Fig. 8 D). Incomplete tagging of adult blood with GFP suggests either variegated CD41-Cre transgene expression (Festenstein et al., 1996) or variable levels of CD41 expression in the developing HSCs. Flow cytometric analysis showed proportionate GFP labeling of lymphoid and myeloid compartments (Fig. 8 E). Southern blot analysis confirmed that GFP-negative blood and bone marrow cells lacked Cre-mediated deletion of the stop cassette (Fig. S8 B). Although GFP expression looks highly specific for blood in the embryo, we wanted to exclude the possibility of illegitimate expression of Cre recombinase in the endothelial population. Although real-time PCR analysis readily identified Cre message in sorted CD41$^+$ cells, it was absent in VE-cad$^+$CD45$^-$CD41$^-$ endothelial cells (Fig. S8 A).

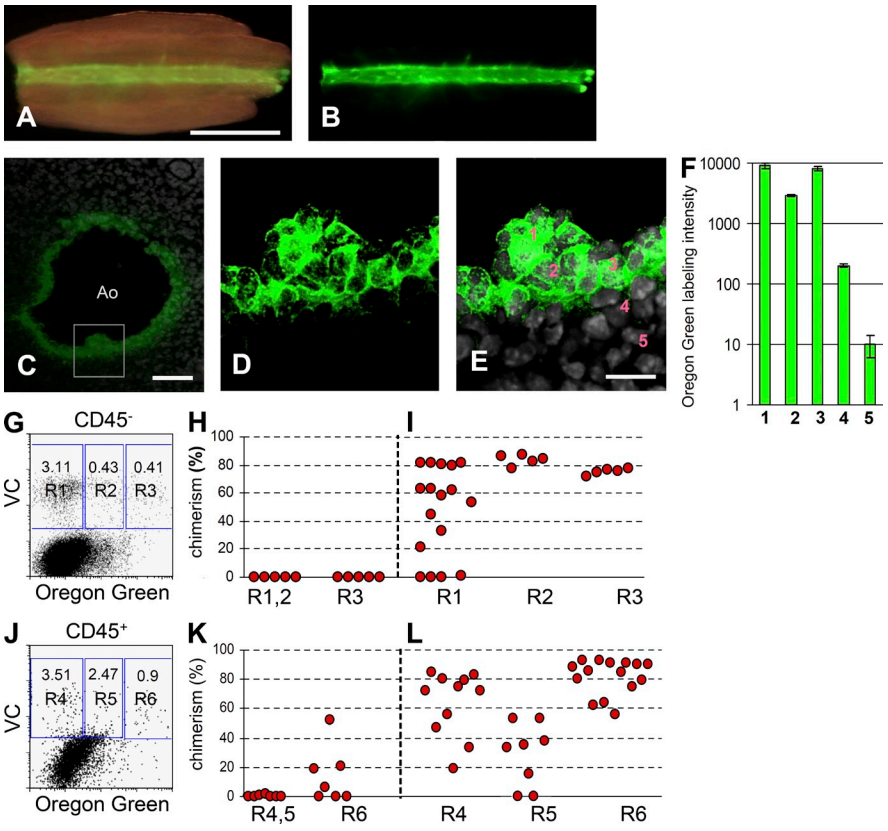

Figure 6. Definitive HSCs are localized to the luminal aortic layer, and pre-HSCs are localized to both the endothelial and deeper subendothelial layers. (A and B) Whole-mount preparation of the E11.5 AGM region labeled with OG. (C) Transverse section of OG-labeled E11.5 dorsal aorta (Ao). The intra-aortic cluster is shown in the boxed area. (D and E) Zoomed image of this cluster and aortic endothelium labeled with OG (D) and counter staining with DAPI (E). Bars: (A and B) 700 µm; (C) 50 µm; (D and E) 20 µm. (F) The intensity of fluorescence of cells labeled 1–5 was assessed and plotted as a histogram. Error bars show standard deviations of intensity of fluorescence from five independent confocal images. (G and J) Gating strategy of VE-cad$^+$CD45$^-$ (G) and VE-cad$^+$CD45$^+$ (J) cell populations isolated from the E11.5 AGM region on the basis of OG labeling. (H, I, K, and L) Transplantation of freshly isolated cells (H and K) and cells cultured in coaggregate with OP9 stromal cells (I and L). R1, VE-cad$^+$CD45$^-$OG$^-$ cells. R2, VE-cad$^+$CD45$^-$OG^{low} cells. R3, VE-cad$^+$CD45$^-$OG^{high} cells. R4, VE-cad$^+$CD45$^+$OG$^-$ cells. R5, VE-cad$^+$CD45$^+$OG^{low} cells. R6, VE-cad$^+$CD45$^+$OG^{high} cells. Dose transplanted was 4 ee/recipient (H and K) and 1 ee/recipient (I and L). Data are derived from two (G–I) or three (J–L) independent experiments. VC, VE-cad.

CD41-Cre transgene expression labels type I pre-HSCs in the E11.5 AGM region

We tested whether CD41-Cre–mediated recombination occurs in pre-HSCs. To this end, we purified GFP$^+$ and GFP$^-$ fractions of VE-cad$^+$CD45$^-$ cells from E11.5 AGM regions of CD41-Cre::sGFP embryos and coaggregated them with OP9 stroma. After 4 d of culture, cells were transplanted into irradiated adult recipients (Fig. 8 B). We found that both GFP$^-$ and GFP$^+$ fractions provided multilineage long-term engraftment. Of note, transplanted HSCs derived from GFP$^-$ pre-HSCs kept generating nonrecombined lymphomyeloid progeny (Fig. 8 B). In contrast, GFP$^+$ pre-HSCs gave rise to HSCs that continued long-term production of GFP$^+$ lymphomyeloid cells in recipient animals. To determine whether Cre-mediated labeling of the type I pre-HSCs translates in vivo into labeling of fetal liver definitive HSCs, we purified GFP$^+$ and GFP$^-$ subsets of the E16.5 fetal liver CD45$^+$CD150$^+$CD48$^-$Ter119$^-$ population and tested them in a long-term repopulation assay. Both GFP$^+$ and GFP$^-$ cell fractions provided long-term multilineage hematopoietic repopulation (Fig. 8 C).

DISCUSSION

A significant body of evidence indicates that the embryonic endothelium of the dorsal aorta is hematogenic (Jaffredo et al., 1998; Nishikawa et al., 1998a,b; Oberlin et al., 2002). Live imaging in zebra fish enabled endothelial-hematopoietic transition to be tracked (Bertrand et al., 2010; Kissa and Herbomel, 2010). Cells of the progenitor/HSC phenotype have been shown to migrate inside the aorta in slices of the cultured AGM region (Boisset et al., 2010). Our present data using OG labeling of the luminal cell layer of the mouse dorsal aorta confirm the previously demonstrated luminal localization of definitive HSCs (de Bruijn et al., 2002). It is thought that intra-aortic clusters are a morphological manifestation of HSCs budding from the endothelial lining of the dorsal aorta (North et al., 1999; Zovein et al., 2008; Chen et al., 2009). Recent identification of pre-HSCs (embryonic ancestors of definitive HSCs) localized to intra-aortic clusters according to phenotypic criteria supports this idea (Taoudi et al., 2008). Some studies, based on indirect evidence, proposed that definitive HSCs may originate from subendothelial layers of the dorsal aorta (North et al., 1999, 2002; Bertrand et al., 2005). However, this idea has mainly been abandoned in favor of direct conversion of endothelial cells into definitive HSCs (e.g., Boisset et al., 2010).

Using an AGM reaggregation system, we previously found that pre-HSCs in the E11.5 AGM region capable of maturing into definitive HSCs coexpress both VE-cad and CD45. Large intra-aortic clusters containing VE-cad$^+$CD45$^+$ cells possess morphological features of active endothelial invagination into the lumen of the dorsal aorta (Taoudi et al., 2008). However, because these pre-HSCs express the principal hematopoietic marker CD45, they cannot be considered to be endothelial cells. Therefore, we have been looking to track the development

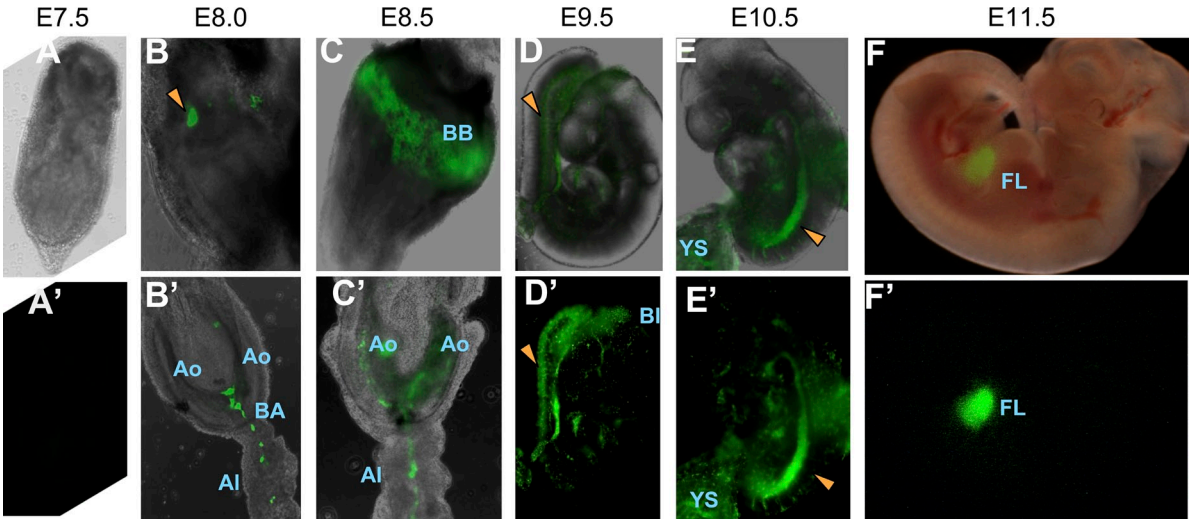

Figure 7. Analysis of CD41-Cre::sGFP embryos. The developing HSC lineage passes through a CD41-positive stage in vivo. (A and A′) E7.5 embryo. (B and B′) E8.0 embryo. GFP$^+$ cells in the YS are indicated by the arrowhead (B) and at the base of the allantois (BA), at the bifurcation of the paired dorsal aorta (Ao), and the allantois (Al) itself (B′). (C and C′) E8.5 embryo. GFP$^+$ cells are within the blood island/belt (BB), allantois, and paired dorsal aorta (C) and within the body of the embryo dissected from the YS (C′). (D and D′) E9.5 embryo. GFP$^+$ cells are in circulation in the dorsal aorta (arrowheads). Bl, blood coming out of the dissected embryo. (E and E′) E10.5 embryo. GFP$^+$ cells in the embryo vasculature. Arrowheads point to the dorsal aorta. (F and F′) E11.5 embryo. GFP$^+$ cells in the liver (FL). A′, D′, E′, and F′ are fluorescent images; A, B, B′, C, C′, D, E, and F are fluorescent images merged with phase-contrast or brightfield images.

of HSCs from true endothelial cells. The use of the complete AGM reaggregation system for this goal was problematic because, although on occasions we observed development of definitive HSCs from CD45$^-$ cells, these might have derived from contaminating VE-cad$^+$CD45$^+$ pre-HSCs (Taoudi et al., 2008).

By replacing the complex AGM microenvironment with the OP9 stromal cell line, we established conditions supporting the development of definitive HSCs predominantly from the VE-cad$^+$CD45$^-$ population. It is possible that the newborn origin of the OP9 line (Nakano et al., 1994) makes them competent to support efficient maturation of pre-HSCs. Our preliminary data show that selected cell lines from the AGM region can also support maturation of type I pre-HSCs into definitive HSCs (unpublished data). We explored the lineage hierarchy between two classes of pre-HSCs (VE-cad$^+$CD45$^-$ and VE-cad$^+$CD45$^+$) and definitive HSCs. Because definitive HSCs in the early embryo are VE-cad$^+$CD45$^+$ (North et al., 2002; Taoudi et al., 2005), their maturation from VE-cad$^+$CD45$^-$ pre-HSCs is likely to be accompanied by acquisition of the CD45 marker. Using a resorting and reculturing strategy, we established that the VE-cad$^+$CD45$^-$ pre-HSCs (type I) mature into the VE-cad$^+$CD45$^+$ pre-HSCs (type II) during the first 24 h of culture. This confirmed that type I pre-HSCs are more immature precursors of type II pre-HSCs.

Using intra-aortic labeling with fluorescent OG dye, we determined that, in contrast to definitive HSCs, a significant proportion of both classes of pre-HSCs are localized to deeper layers of the dorsal aorta. We also found that although at all maturation steps the HSC lineage starting from type I pre-HSCs are marked by VE-cad, they are also marked by hematopoietic markers, first by CD41 in type I pre-HSCs and slightly later by CD45 in type II pre-HSCs and definitive HSCs. Interestingly, CD41 expression was found in E9.5–10.5 embryonic cells capable of long-term contribution into adult hematopoiesis upon transplantation into newborn recipients (Yoder et al., 1997; Ferkowicz et al., 2003). Our experiments demonstrate that the VE-cad$^+$CD45$^-$CD41$^+$ cells, in contrast to the VE-cad$^+$CD45$^-$CD41$^-$ population, do not form endothelial colonies in vitro, which is in agreement with previous studies (Li et al., 2005; Hashimoto et al., 2007). The lack of endothelial potential and priming with the CD41 hematopoietic marker shows that type I pre-HSCs are not endothelial cells.

One of us previously generated CD41-Cre mice and by crossing with silent Rosa26-LacZ mice reported extensive Cre-mediated labeling of embryonic but not adult blood (Emambokus and Frampton, 2003). In this study, we used sGFP reporter mice (Gilchrist et al., 2003) and found considerable (35–65%) labeling of the adult hematopoietic system. It is likely that in the previous model a low level of LacZ expression in adult hematopoietic cells went unnoticed. GFP labeling is observed in type I pre-HSCs in the E11.5 AGM region in a ratio similar to the labeling of HSCs in the fetal liver and of the adult hematopoietic system. This confirms that type I pre-HSCs are true in vivo embryonic precursors of the adult hematopoietic system. Partial recombination in the hematopoietic system may be a result of a slightly lower level of CD41 expression in a fraction of pre-HSCs/definitive HSCs or because of variegated transgene expression (Festenstein et al., 1996).

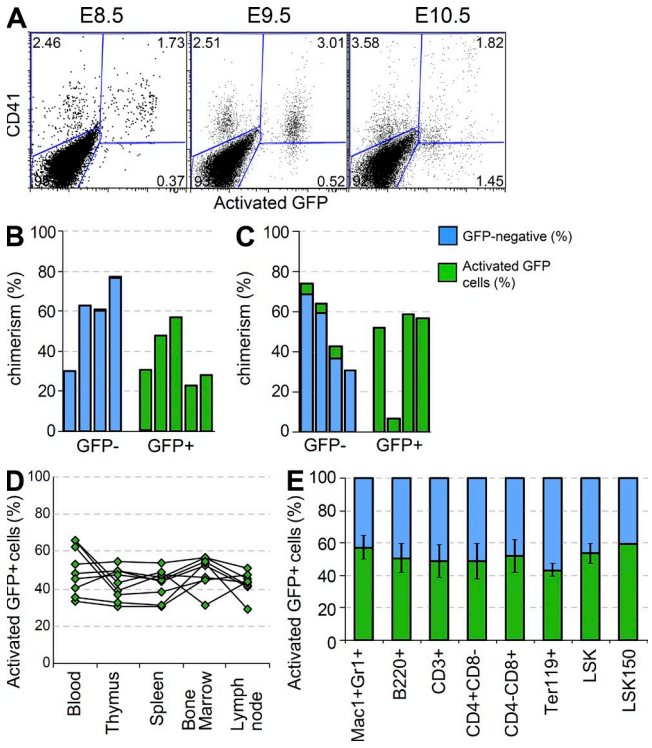

Figure 8. Level of CD41-Cre–mediated recombination throughout development. (A) GFP expression in the embryonic CD41$^+$ population (gated on CD45$^-$ live cells). (B) GFP$^+$VE-cad$^+$CD45$^-$ and GFP$^-$VE-cad$^+$CD45$^-$ populations were purified from E11.5 AGM regions and co-aggregated with OP9 cells. After 4 d of co-culture, 0.5 ee of donor-derived cells were transplanted per recipient (each recipient is represented by one bar). Analysis of donor-derived blood cells was performed at 3.5 mo. Data are derived from two experiments. (C) GFP$^+$ and GFP$^-$ subsets of CD150$^+$CD45$^+$CD48$^-$Ter119$^-$ cells were sorted from E16.5 fetal livers and transplanted (100 cells/recipient) directly after sorting. Donor-derived blood chimerism was assessed 3.5 mo after transplantation. Each bar represents one recipient. (D) Proportion of GFP$^+$ cells (percentage) in blood and hematopoietic organs of adult CD41-Cre::sGFP animals. (E) Proportion of GFP$^+$ cells (percentage) in different hematopoietic lineages of adult bone marrow. LSK, lineage-negative cKit$^+$Sca1$^+$ cells. LSK150, Lin$^-$Sca1$^+$cKit$^+$CD48$^-$CD34$^{low/-}$CD150$^+$ cells. Each experiment was replicated twice. Error bars show standard deviation (five mice).

The simplest model of HSC development emerging from our experiments suggests that hematopoietically committed type I pre-HSCs mature into type II pre-HSCs in both the subluminal and luminal layers of the dorsal aorta but that the final maturation step resulting in the formation of definitive HSCs occurs exclusively within the endothelial lining of the dorsal aorta (Fig. S8 C). This model suggests a temporary integration of the hematopoietically committed HSC lineage into the aortic endothelial layer by E11.5, perhaps facilitated by VE-cad expression (Breviario et al., 1995; Carmeliet et al., 1999). Although previously discussed in the literature (North et al., 1999; North et al., 2002; Bertrand et al., 2005), this scenario has mainly been abandoned in favor of a direct one-step appearance of definitive HSCs from the E10–11.5 aortic endothelium. Our model does not exclude the endothelial origin of the HSC lineage (Eilken et al., 2009; Lancrin et al., 2009; Kissa and Herbomel, 2010) but outlines a more complex three-step scenario. Early priming of the HSC lineage with CD41 beginning from E9.5 (Ferkowicz et al., 2003) indicates that segregation of the HSC lineage from the endothelial compartment occurs well before the emergence of definitive HSCs in E11.5 embryos. However, the specification of the HSC lineage from the subendothelial Runx1-expressing mesenchyme cannot be excluded either (North et al., 1999, 2002). Indicatively, the subaortic mesenchyme in amphibians exhibits expression of key hematopoietic transcription factors (SCL, Runx1, and Gata2; Ciau-Uitz et al., 2000). More complex scenarios are conceivable. For example, it cannot be excluded that the remodeling endothelial network beneath the dorsal aorta, including omphalomesenteric artery, is a source of subaortic pre-HSCs (Zovein et al., 2010). If so, pre-HSCs from these vessels migrate toward the dorsal aorta where they become definitive HSCs. Interestingly, we have not been able to detect type I pre-HSCs in the YS. Identification of the developmental stage preceding the formation of type I pre-HSCs in the AGM region is an important issue that will pose a significant challenge for further research.

In summary, the identification of two classes of hematopoietically primed pre-HSCs, which are broadly distributed through the wall of the dorsal aorta, unveils a more complex picture of definitive HSC formation than a one-step model of HSC origin from the E11.5 aortic endothelium. Together with a previous publication (Ferkowicz et al., 2003), our data indicate that the definitive HSC lineage is hematopoietically primed from very early stages. The dispersed spatial distribution of pre-HSCs and restricted luminal location of definitive HSCs suggest centripetal migration of the maturing pre-HSC lineage from the subluminal area of the dorsal aorta before entry into circulation.

MATERIALS AND METHODS

Mice. Mice were maintained and bred in compliance with UK Home Office regulations. C57BL/6 (*CD45.2/2*) or C57BL/6-EGFP (Gilchrist et al., 2003) were paired to generate embryos of appropriate stage. The morning of discovery of the vaginal plug was designated as day 0.5. E10.S embryos used were 36–39 somite pairs. E11.5 embryos used were 41–45 somite pairs. C57BL/6 (*CD45.1/CD45.1*) animals were used as recipients. All experiments with animals were approved under a Project License granted by the Home Office (UK), University of Edinburgh Ethical Review Committee, and conducted in accordance with local guidelines.

FACS. E11.5 AGM regions were dissected and dissociated as previously described (Medvinsky et al., 2008). The following antibodies (BD) were used for staining of cells: anti-CD45-FITC or anti-CD45-APC (clone 30-F11), anti-CD41-PE (clone MW30reg), and biotinylated anti–VE-cad (clone 11.D4.1), followed by incubation with streptavidin-APC or PE. Cell populations were isolated using a MoFlo cell sorter (Cytomation). Hematopoietic lineage depletion was performed using a cocktail of antibodies (anti–mouse-B220, -CD19, -CD4, -CD8, -CD3, -Mac1, -Gr1, and -Ter119 antibodies conjugated with PE). Anti–mouse VE-cad antibody was biotinylated according to the manufacturer's protocol (FluoReporter Mini-bio-XX; Invitrogen). Purity checks were performed on aliquots from the collected samples. Gating of negative populations was performed on the basis of isotype control staining (BD). In cases of three-color analysis, fluorescence minus one stainings

were used as negative controls: one of the antibodies was substituted with an appropriate isotype control. In all analyses and sorting, live gating was performed on the basis of 7AAD exclusion. All FACS plots are presented in logarithmic scale.

Long-term hematopoietic repopulation assays. Cells sorted from *CD45.2/2* (or *GFP*$^+$) embryos were injected into irradiated adult recipients (*CD45.1/1*) either directly or after co-culture with OP9 cells along with 20,000 *CD45.2/1* bone marrow carrier cells. Recipients were irradiated by split dose (600 + 550 rad with 3-h interval) of γ irradiation. The numbers of cells of a particular cell population are expressed throughout the article in doses, defined as embryo equivalent, which corresponds to the number of given cells in one AGM region (for example, 0.2-ee dose is equal to 20% of a given cell population present in one AGM region). Donor-derived chimerism was monitored in blood at 6.5 wk, 14 wk, and 12 mo after transplantation using FACScalibur (BD). The peripheral blood was collected by bleeding the lateral tail vein into 500 µl EDTA/PBS, and erythrocytes were depleted using PharM Lyse (BD). Cells were stained with anti-CD16/32 (Fc-block), anti-CD45.1-FITC or CD45.1-APC (clone A20), and anti-CD45.2-PE (clone 104) monoclonal antibodies (eBioscience). Appropriate isotype controls were used. Dead cells were excluded using 7AAD (eBioscience). Mice demonstrating ≥5% donor-derived multilineage chimerism after 14 wk were considered to be reconstituted. Calculation of HSC numbers was performed using regression analysis based on the data obtained in limiting dilution experiments (Szilvassy et al., 1990; Kumaravelu et al., 2002). When 37% of mice are nonrepopulated in a group receiving a particular dose, this corresponds statistically to 1 definitive HSC transplanted on average per mouse (Fig. 2 E).

In recipient animals, donor-derived contribution into different hematopoietic lineages in blood or organs was determined by gating on GFP$^+$ cells or by exclusion of recipient CD45.1$^+$ cells and staining with lineage-specific monoclonal antibodies for Mac1, CD3e, CD4, CD41, Gr1, B220, CD8, and Ter119. Antibodies were conjugated with PE, FITC, APC, or biotin. Biotinylated antibodies were detected by incubation with streptavidin APC or PE (BD). Staining of CD41$^+$ cells for sorting was performed always using PE-conjugated antibody. All analyses were performed using FlowJo software (Tree Star).

Culture of embryonic cells in coaggregates with OP9 cells. The cell populations sorted from one AGM region were mixed with 10^5 OP9 cells and centrifuged as previously described (Taoudi et al., 2008; Sheridan et al., 2009). In brief, to prepare one coaggregate the cell mixture containing 1 ee of AGM cells and OP9 cells was suspended in 30 µl of IMDM$^+$ media, aspirated in a yellow tip, sealed with parafilm, and centrifuged at 400 *g* for 5 min at room temperature. The coaggregates were transferred onto 0.65-µm Durapore membranes (Millipore). OP9-AGM cell coaggregates were cultured at the liquid–gas interface with IMDM$^+$ media consisting of IMDM (Invitrogen) and growth factors (100 ng/ml IL-3, 100 ng/ml SCF, and 100 ng/ml Flt3 ligand; all from PeproTech) supplemented with L-glutamine and penicillin/streptomycin. After 4 d, aggregates were dissociated as previously described (Taoudi et al., 2008). The majority of aggregate cultures followed by long-term repopulation experiments were performed two or more times.

Single-cell deposition analysis. AGM region VE-cad$^+$CD45$^-$ cells were sorted on the basis of CD41$^+$ or CD41$^-$ expression, and individual cells were deposited in 96-well plates with the layer of OP9 cells and overlayed with methylcellulose (MethoCult3434 medium; STEMCELL Technologies) containing 100 ng/ml IL-3, SCF, and Flt3l and 50 ng/ml vascular endothelial growth factor (all from PeproTech). After 9 and 11 d, cultures were stained with anti-CD45 and anti-CD31 antibodies, and colonies were counted.

Confocal microscopy. AGM regions were dissected and embedded in OCT by flash freezing samples on dry ice. 10-µm transverse sections were produced using a CM1900 cryostat (Leica) and processed as previously described (Taoudi and Medvinsky, 2007). Images were captured using an upright confocal microscope (DM IRE2; Leica) and processed using Photoshop CS2 (Adobe) or European Molecular Biology Laboratory ImageJ (National Institutes of Health). Sections were fixed by cold acetone, rehydrated with PBS, and blocked by 20% FCS. Staining with goat anti–mouse CD45 (clone AF114; R&D Systems) and directly conjugated rat anti–mouse–VE-cad–Alexa Fluor 647 (clone eBioBV13; BioLegend) was followed by incubation with secondary rabbit anti–goat IgG–Alexa Fluor 488 antibody (Invitrogen). After washing with PBS, the sections were incubated with nonimmune goat serum to block nonspecific binding followed by incubation with the goat anti–rat Ig–Alexa Fluor 633 (Invitrogen) and followed by further washing with PBS. After that the sections were incubated with Fc blocking reagent followed by fixation with 5% paraformaldehyde and incubation with anti–mouse CD41-PE (clone MWreg30; BD). In some cases, instead of using goat anti–mouse CD45, directly conjugated rat anti–mouse CD45–Alexa Flour 488 (clone 30-F11; BioLegend) was used. Sections were counterstained with DAPI.

OG 488 staining. Stock solution was prepared by dissolving 0.5 mM OG 488 Cell Trace (Invitrogen) in 169 µl DMSO. To obtain 1-µM staining solution, 2 µl of stock was diluted in 1 ml PBS. We determined that 1-µM solution of OG optimally stained all cells in the AGM cell suspension during 30 s (Fig. S5 A). Furthermore, all pre-HSCs were also labeled with 1 µM OG solution in cell suspension (Fig. S5 B). This concentration of OG was chosen for further experiments.

E11.5 embryos were decapitated immediately above forelimbs and cut through hind limbs to open the caudal part of the dorsal aorta. OG solution was injected by mouth micropipette into the dorsal aorta and washed out after 30 s by injection of PBS supplemented with 20% FCS. After that, the embryo was additionally washed, and the AGM region was dissected. After dissociation of the AGM region, the cells were stained with antibodies for flow cytometry. Intensity of fluorescence of OG on sections was measured using DM IRE2 software (Leica).

Online supplemental material. Fig. S1 shows E11.5 AGM cell sorting and typical purity of sorted populations. Fig. S2 shows multilineage long-term engraftment of primary and secondary recipients transplanted with definitive HSCs developed from AGM E11.5 VE-cad$^+$CD45$^-$ pre-HSCs (type I) after 4-d co-culture with OP9 cells. Fig. S3 shows that pre-HSC type I populations develop into pre-HSC type II populations before maturing into definitive HSCs. Fig. S4 shows that pre-HSCs are VE-cad$^+$CD45$^-$Lin$^-$. Fig. S5 shows the titration of OG 488. Fig. S6 shows localization of candidate type I (VE-cad$^+$CD45$^-$CD41$^+$) cells in the dorsal aorta. Fig. S7 shows localization of candidate type II (VE-cad$^+$CD45$^+$) pre-HSCs in the dorsal aorta. Fig. S8 shows the characterization of CD41-Cre–mediated recombination. Online supplemental material is available at http://www.jem.org/cgi/content/full/jem.20102419/DC1.

We thank C. Manson and J. Verth for animal maintenance and recipient irradiation, J. Vrana and S. Monard for cell sorting, A. Wilson (École Polytechnique Federale de Lausanne, Lausanne, Switzerland) for advice with multicolor flow cytometric analysis, and S. Gordon-Keylock for useful comments on the manuscript.

This research was supported by funding from Leukaemia and Lymphoma Research, the Biotechnology and Biological Sciences Research Council, the Medical Research Council, and the Fundación Alfonso Martín Escudero.

The authors declare no financial conflicts of interest.

Submitted: 18 November 2010
Accepted: 27 April 2011

REFERENCES

Bertrand, J.Y., S. Giroux, R. Golub, M. Klaine, A. Jalil, L. Boucontet, I. Godin, and A. Cumano. 2005. Characterization of purified intraembryonic hematopoietic stem cells as a tool to define their site of origin. *Proc. Natl. Acad. Sci. USA*. 102:134–139. doi:10.1073/pnas.0402270102

Bertrand, J.Y., N.C. Chi, B. Santoso, S. Teng, D.Y. Stainier, and D. Traver. 2010. Haematopoietic stem cells derive directly from aortic endothelium during development. *Nature*. 464:108–111. doi:10.1038/nature08738

Boisset, J.C., W. van Cappellen, C. Andrieu-Soler, N. Galjart, E. Dzierzak, and C. Robin. 2010. In vivo imaging of haematopoietic

cells emerging from the mouse aortic endothelium. *Nature*. 464:116–120. doi:10.1038/nature08764

Breviario, F., L. Caveda, M. Corada, I. Martin-Padura, P. Navarro, J. Golay, M. Introna, D. Gulino, M.G. Lampugnani, and E. Dejana. 1995. Functional properties of human vascular endothelial cadherin (7B4/cadherin-5), an endothelium-specific cadherin. *Arterioscler. Thromb. Vasc. Biol*. 15:1229–1239.

Cai, Z., M. de Bruijn, X. Ma, B. Dortland, T. Luteijn, R.J. Downing, and E. Dzierzak. 2000. Haploinsufficiency of AML1 affects the temporal and spatial generation of hematopoietic stem cells in the mouse embryo. *Immunity*. 13:423–431. doi:10.1016/S1074-7613(00)00042-X

Carmeliet, P., M.G. Lampugnani, L. Moons, F. Breviario, V. Compernolle, F. Bono, G. Balconi, R. Spagnuolo, B. Oosthuyse, M. Dewerchin, et al. 1999. Targeted deficiency or cytosolic truncation of the VE-cadherin gene in mice impairs VEGF-mediated endothelial survival and angiogenesis. *Cell*. 98:147–157. doi:10.1016/S0092-8674(00)81010-7

Chen, M.J., T. Yokomizo, B.M. Zeigler, E. Dzierzak, and N.A. Speck. 2009. Runx1 is required for the endothelial to haematopoietic cell transition but not thereafter. *Nature*. 457:887–891. doi:10.1038/nature07619

Ciau-Uitz, A., M. Walmsley, and R. Patient. 2000. Distinct origins of adult and embryonic blood in *Xenopus*. *Cell*. 102:787–796. doi:10.1016/S0092-8674(00)00067-2

Corbel, C., and J. Salaün. 2002. AlphaIIb integrin expression during development of the murine hemopoietic system. *Dev. Biol*. 243:301–311. doi:10.1006/dbio.2001.0553

de Bruijn, M.F.T.R., X. Ma, C. Robin, K. Ottersbach, M.-J. Sanchez, and E. Dzierzak. 2002. Hematopoietic stem cells localize to the endothelial cell layer in the midgestation mouse aorta. *Immunity*. 16:673–683. doi:10.1016/S1074-7613(02)00313-8

Dzierzak, E., and N.A. Speck. 2008. Of lineage and legacy: the development of mammalian hematopoietic stem cells. *Nat. Immunol*. 9:129–136. doi:10.1038/ni1560

Eilken, H.M., S. Nishikawa, and T. Schroeder. 2009. Continuous single-cell imaging of blood generation from haemogenic endothelium. *Nature*. 457:896–900. doi:10.1038/nature07760

Emambokus, N.R., and J. Frampton. 2003. The glycoprotein IIb molecule is expressed on early murine hematopoietic progenitors and regulates their numbers in sites of hematopoiesis. *Immunity*. 19:33–45. doi:10.1016/S1074-7613(03)00173-0

Ferkowicz, M.J., M. Starr, X. Xie, W. Li, S.A. Johnson, W.C. Shelley, P.R. Morrison, and M.C. Yoder. 2003. CD41 expression defines the onset of primitive and definitive hematopoiesis in the murine embryo. *Development*. 130:4393–4403. doi:10.1242/dev.00632

Festenstein, R., M. Tolaini, P. Corbella, C. Mamalaki, J. Parrington, M. Fox, A. Miliou, M. Jones, and D. Kioussis. 1996. Locus control region function and heterochromatin-induced position effect variegation. *Science*. 271:1123–1125. doi:10.1126/science.271.5252.1123

Gilchrist, D.S., J. Ure, L. Hook, and A. Medvinsky. 2003. Labeling of hematopoietic stem and progenitor cells in novel activatable EGFP reporter mice. *Genesis*. 36:168–176. doi:10.1002/gene.10209

Godin, I., and A. Cumano. 2002. The hare and the tortoise: an embryonic haematopoietic race. *Nat. Rev. Immunol*. 2:593–604.

Hashimoto, K., T. Fujimoto, Y. Shimoda, X. Huang, H. Sakamoto, and M. Ogawa. 2007. Distinct hemogenic potential of endothelial cells and CD41+ cells in mouse embryos. *Dev. Growth Differ*. 49:287–300. doi:10.1111/j.1440-169X.2007.00925.x

Jaffredo, T., R. Gautier, A. Eichmann, and F. Dieterlen-Lièvre. 1998. Intraaortic hemopoietic cells are derived from endothelial cells during ontogeny. *Development*. 125:4575–4583.

Kissa, K., and P. Herbomel. 2010. Blood stem cells emerge from aortic endothelium by a novel type of cell transition. *Nature*. 464:112–115. doi:10.1038/nature08761

Kumaravelu, P., L. Hook, A.M. Morrison, J. Ure, S. Zhao, S. Zuyev, J. Ansell, and A. Medvinsky. 2002. Quantitative developmental anatomy of definitive haematopoietic stem cells/long-term repopulating units (HSC/RUs): role of the aorta-gonad-mesonephros (AGM) region and the yolk sac in colonisation of the mouse embryonic liver. *Development*. 129:4891–4899.

Lancrin, C., P. Sroczynska, C. Stephenson, T. Allen, V. Kouskoff, and G. Lacaud. 2009. The haemangioblast generates haematopoietic cells through a haemogenic endothelium stage. *Nature*. 457:892–895. doi:10.1038/nature07679

Li, W., M.J. Ferkowicz, S.A. Johnson, W.C. Shelley, and M.C. Yoder. 2005. Endothelial cells in the early murine yolk sac give rise to CD41-expressing hematopoietic cells. *Stem Cells Dev*. 14:44–54. doi:10.1089/scd.2005.14.44

McKinney-Freeman, S.L., O. Naveiras, F. Yates, S. Loewer, M. Philitas, M. Curran, P.J. Park, and G.Q. Daley. 2009. Surface antigen phenotypes of hematopoietic stem cells from embryos and murine embryonic stem cells. *Blood*. 114:268–278. doi:10.1182/blood-2008-12-193888

Medvinsky, A., and E. Dzierzak. 1996. Definitive hematopoiesis is autonomously initiated by the AGM region. *Cell*. 86:897–906. doi:10.1016/S0092-8674(00)80165-8

Medvinsky, A., S. Taoudi, S. Mendes, and E. Dzierzak. 2008. Analysis and manipulation of hematopoietic progenitor and stem cells from murine embryonic tissues. *Curr. Protoc. Stem Cell Biol*. Chapter 2:2A: 6.

Medvinsky, A., S. Rybtsov, and S. Taoudi. 2011. Embryonic origin of the adult hematopoietic system: advances and questions. *Development*. 138:1017–1031. doi:10.1242/dev.040998

Mikkola, H.K., Y. Fujiwara, T.M. Schlaeger, D. Traver, and S.H. Orkin. 2003. Expression of CD41 marks the initiation of definitive hematopoiesis in the mouse embryo. *Blood*. 101:508–516. doi:10.1182/blood-2002-06-1699

Müller, A.M., A. Medvinsky, J. Strouboulis, F. Grosveld, and E. Dzierzak. 1994. Development of hematopoietic stem cell activity in the mouse embryo. *Immunity*. 1:291–301. doi:10.1016/1074-7613(94)90081-7

Nakano, T., H. Kodama, and T. Honjo. 1994. Generation of lymphohematopoietic cells from embryonic stem cells in culture. *Science*. 265:1098–1101. doi:10.1126/science.8066449

Nishikawa, S.I., S. Nishikawa, M. Hirashima, N. Matsuyoshi, and H. Kodama. 1998a. Progressive lineage analysis by cell sorting and culture identifies FLK1+VE-cadherin+ cells at a diverging point of endothelial and hemopoietic lineages. *Development*. 125:1747–1757.

Nishikawa, S.I., S. Nishikawa, H. Kawamoto, H. Yoshida, M. Kizumoto, H. Kataoka, and Y. Katsura. 1998b. In vitro generation of lymphohematopoietic cells from endothelial cells purified from murine embryos. *Immunity*. 8:761–769. doi:10.1016/S1074-7613(00)80581-6

North, T., T.L. Gu, T. Stacy, Q. Wang, L. Howard, M. Binder, M. Marín-Padilla, and N.A. Speck. 1999. Cbfa2 is required for the formation of intra-aortic hematopoietic clusters. *Development*. 126:2563–2575.

North, T.E., M.F. de Bruijn, T. Stacy, L. Talebian, E. Lind, C. Robin, M. Binder, E. Dzierzak, and N.A. Speck. 2002. Runx1 expression marks long-term repopulating hematopoietic stem cells in the midgestation mouse embryo. *Immunity*. 16:661–672. doi:10.1016/S1074-7613(02)00296-0

Oberlin, E., M. Tavian, I. Blazsek, and B. Péault. 2002. Blood-forming potential of vascular endothelium in the human embryo. *Development*. 129:4147–4157.

Robin, C., K. Ottersbach, C. Durand, M. Peeters, L. Vanes, V. Tybulewicz, and E. Dzierzak. 2006. An unexpected role for IL-3 in the embryonic development of hematopoietic stem cells. *Dev. Cell*. 11:171–180. doi:10.1016/j.devcel.2006.07.002

Sheridan, J.M., S. Taoudi, A. Medvinsky, and C.C. Blackburn. 2009. A novel method for the generation of reaggregated organotypic cultures that permits juxtaposition of defined cell populations. *Genesis*. 47:346–351. doi:10.1002/dvg.20505

Szilvassy, S.J., R.K. Humphries, P.M. Lansdorp, A.C. Eaves, and C.J. Eaves. 1990. Quantitative assay for totipotent reconstituting hematopoietic stem cells by a competitive repopulation strategy. *Proc. Natl. Acad. Sci. USA*. 87:8736–8740. doi:10.1073/pnas.87.22.8736

Taoudi, S., and A. Medvinsky. 2007. Functional identification of the hematopoietic stem cell niche in the ventral domain of the embryonic dorsal aorta. *Proc. Natl. Acad. Sci. USA*. 104:9399–9403. doi:10.1073/pnas.0700984104

Taoudi, S., A.M. Morrison, H. Inoue, R. Gribi, J. Ure, and A. Medvinsky. 2005. Progressive divergence of definitive haematopoietic stem cells from the endothelial compartment does not depend on contact with the foetal liver. *Development*. 132:4179–4191. doi:10.1242/dev.01974

Taoudi, S., C. Gonneau, K. Moore, J.M. Sheridan, C.C. Blackburn, E. Taylor, and A. Medvinsky. 2008. Extensive hematopoietic stem cell generation

in the AGM region via maturation of VE-cadherin+CD45+ pre-definitive HSCs. *Cell Stem Cell*. 3:99–108. doi:10.1016/j.stem.2008.06.004

Yoder, M.C., K. Hiatt, P. Dutt, P. Mukherjee, D.M. Bodine, and D. Orlic. 1997. Characterization of definitive lymphohematopoietic stem cells in the day 9 murine yolk sac. *Immunity*. 7:335–344. doi:10.1016/S1074-7613(00)80355-6

Yokomizo, T., and E. Dzierzak. 2010. Three-dimensional cartography of hematopoietic clusters in the vasculature of whole mouse embryos. *Development*. 137:3651–3661. doi:10.1242/dev.051094

Zovein, A.C., J.J. Hofmann, M. Lynch, W.J. French, K.A. Turlo, Y. Yang, M.S. Becker, L. Zanetta, E. Dejana, J.C. Gasson, et al. 2008. Fate tracing reveals the endothelial origin of hematopoietic stem cells. *Cell Stem Cell*. 3:625–636. doi:10.1016/j.stem.2008.09.018

Zovein, A.C., K.A. Turlo, R.M. Ponec, M.R. Lynch, K.C. Chen, J.J. Hofmann, T.C. Cox, J.C. Gasson, and M.L. Iruela-Arispe. 2010. Vascular remodeling of the vitelline artery initiates extravascular emergence of hematopoietic clusters. *Blood*. 116:3435–3444. doi:10.1182/blood-2010-04-279497